European Journal of Medicinal Chemistry 216 (2021) 113285

Contents lists available at ScienceDirect

European Journal of Medicinal Chemistry

journal homepage: http://www.elsevier.com/locate/ejmech

Tackling resistance in chronic myeloid leukemia: Novel cell death modulators with improved efficacy

Anna M. Schoepf [a, b], Stefan Salcher [c, d], Petra Obexer [c, e], Ronald Gust [a, *]

[a] Department of Pharmaceutical Chemistry, Institute of Pharmacy, CMBI - Center for Molecular Biosciences Innsbruck, University of Innsbruck, CCB - Centrum for Chemistry and Biomedicine, Innrain 80-82, 6020, Innsbruck, Austria
[b] Division of Cancer Therapeutics, The Institute of Cancer Research, London, SM2 5NG, United Kingdom
[c] Tyrolean Cancer Research Institute, Innrain 66, 6020, Innsbruck, Austria
[d] Department of Internal Medicine V, Medical University Innsbruck, Anichstraße 35, 6020, Innsbruck, Austria
[e] Department of Pediatrics II, Medical University Innsbruck, Innrain 66, 6020, Innsbruck, Austria

ARTICLE INFO

Article history:
Received 10 October 2020
Received in revised form
2 February 2021
Accepted 5 February 2021
Available online 18 February 2021

Keywords:
Chronic myeloid leukemia
Imatinib resistance
Cell death modulators
Chemosensitizers
Signal transducer and activator of transcription 5
Peroxisome proliferator-activated receptor γ

ABSTRACT

The development of resistance poses a serious problem in the therapy of cancer due to the necessity of a multiple-drug and unlimited treatment of affected patients. In chronic myeloid leukemia (CML), the introduction of imatinib has revolutionized the therapy. The persistence of an untreatable cancer stem cell pool and other resistance-causing factors, however, also impede the cure of this malignancy. New therapeutic approaches are therefore essential to overcome current treatment drawbacks. In this regard, an intervention in the STAT5 signaling pathway can significantly improve drug response, as this central signaling node induces the formation of highly resistant CML cells. In the present study, we continued the design of efficient chemosensitizers derived from the partial PPARγ agonist telmisartan. The developed 2-carbonitriles or 2-carboxymethyl esters showed improved potency in sensitizing K562-resistant cells to imatinib treatment, even at concentrations, which are considered patient-relevant. At 5 μM, for instance, **2d** sensitized the cells in such a manner that the resistance was fully overcome and the recovered efficacy of imatinib resulted in >76% cell death. Importantly, all compounds were non-cytotoxic *per se*. A transactivation experiment showed that only the carbonitriles are partial agonists of PPARγ, which does not seem to be involved in the mode of action. Yet, immunoassays revealed a suppression of the STAT5 phosphorylation status by co-application of the most active derivatives with imatinib. This mechanism consequently resulted in reduced cell proliferation and induction of cell death in resistant CML cells.

1. Introduction

Although the introduction of tyrosine kinase inhibitors (TKIs) considerably improved the treatment of chronic myeloid leukemia (CML), patients still show suboptimal response and progression of disease. The tumor initiating BCR-ABL fusion gene, which produces the BCR-ABL protein that represents a constitutively active tyrosine kinase, as well as additional genetic mutations maintain the hematological malignancy [1].

While drug resistance most commonly depends on mutations of the BCR-ABL kinase domain, a number of independent mechanisms, e.g. the dysregulation of the signal transducer and activator of transcription 5 (STAT5) or drug transporters, the inhibition of pro-apoptotic proteins, and the development of an insensitive leukemic stem cell (LSC) pool were described [2]. Recent investigations focus on these independent mechanisms of resistance in CML. Hoelbl et al. [3] reported that STAT5 is essential for leukemia initiation and maintenance *in vitro* and *in vivo*. Moreover,

Abbreviations: TKI, tyrosine kinase inhibitor; CML, chronic myeloid leukemia; STAT5, signal transducer and activator of transcription 5; LSCs, leukemic stem cells; OCT1, organic cation transporter 1; PPARγ, peroxisome proliferator-activated receptor gamma; SAR, structure-activity relationship; MTT, 3-(4,5-dimethylthiazol-2-yl)-2,5-diphenyltetrazolium bromide; MeOH, methanol; EA, ethyl acetate; EtOH, ethanol; PE, petroleum ether; eq, equivalents; HRMS, high-resolution mass spectrometry; A_{max}, intrinsic activation; SD, standard deviation; SEM, standard error of the mean; ctr., control; DMEM, Dulbecco's Modified Eagle Medium; FCS, fetal calf serum; RPMI, Roswell Park Memorial Institute; PBS, phosphate-buffered saline; PI, propidium iodide.

* Corresponding author.
E-mail address: ronald.gust@uibk.ac.at (R. Gust).

https://doi.org/10.1016/j.ejmech.2021.113285

persistent activation of this transcription factor was not only found in the majority of hematologic malignancies, but also in solid tumors. Thus, inhibition of STAT5 is a promising therapeutic option, especially since it was identified as the central signaling node in CML [4]. Wang et al. [5] and Yousefi et al. [6,7] studied the impact of specific transporters on the emergence of resistance by a change in intracellular uptake of imatinib or other chemotherapeutics. Besides the controversially discussed organic cation transporter 1 (OCT1) transporter, they evaluated the role of P-glycoprotein-mediated drug resistance in leukemic cells.

Peroxisome proliferator-activated receptor gamma (PPARγ) ligands are capable to influence both STAT5 and the mentioned transporters. Co-treatment of chemotherapeutics with the agonists balaglitazone, pioglitazone, or rosiglitazone enhanced apoptosis as well as cell cycle arrest *via* inhibition of STAT5 or P-glycoprotein in resistant CML cells, although these PPARγ ligands did not affect the cells *per se* [7,8]. Notably, the eradication of the quiescent LSC pool by combining them with first, second, or third generation TKIs was proven [9,10]. Despite the sensitizing effects and the possibility to overcome resistance, a successful applicability and a widespread clinical use of full PPARγ agonists is not feasible. Typical glitazone-like side effects caused a discontinuation of the clinical phase of balaglitazone and led to an early withdrawal of rosiglitazone or others from the market. Merely pioglitazone can be prescribed in the European Union, if certain rules for prescription are followed.

In recent studies, we revealed promising results upon combining the partial PPARγ agonist telmisartan (Fig. 1), which advantageously does not induce glitazone-like side effects, with imatinib in K562-resistant CML cells. The sensitization to imatinib treatment was even beneficial compared to that achieved by pioglitazone [11–13]. Regarding the activation of PPARγ, the 4'-((2-propyl-1*H*-benzo[*d*]imidazol-1-yl)methyl)-[1,1′-biphenyl]-2-carboxylic acid (lead, Fig. 1) was identified as essential part of telmisartan [14]. Within the same structure-activity relationship (SAR) study, the 4'-((**4-methyl**-2-propyl-1*H*-benzo[*d*]imidazol-1-yl)methyl)-[1,1′-biphenyl]-2-carboxylic acid (methyl-lead, Fig. 1) was found to have major impact on partial agonism. Derivatization of the 2-COOH group to an amide, remarkably improved the cell death modulating effects of telmisartan, the lead, and the methyl-lead. Interestingly, this modification strongly reduced the activation of PPARγ [11,12,15] and points to a PPARγ-independent mode of action. Esterification of the lead even caused a nearly complete loss of receptor binding [13].

In continuation of these SAR studies, we synthesized related 4-substituted derivatives of the methyl-lead, resulting in the two new series of carbonitriles (**2a-h**) and carboxymethyl esters (**3a-h**) (Fig. 1). Since the 2-COOH group strongly contribute to a high activation of PPARγ, these derivatizations (esterification or exchange by carbonitrile) were aimed at reducing receptor-induced side effects and simultaneously attaining significant cell death modulation. Based on this intention, we investigated all compounds regarding their PPARγ activity and their potency to sensitize resistant leukemia cells to TKI treatment with imatinib as representative.

All compounds were examined for cytotoxicity in K562-resistant CML cells either alone or in combination with imatinib using propidium iodide (PI) FACS analyses. HS-5 human bone marrow stromal cells were analyzed by PI FACS and COS-7 monkey kidney fibroblast-like cells additionally in a modified MTT assay to study the unspecific cytotoxicity of the synthesized derivatives or their combination with imatinib at the applied concentrations. COS-7 cells were further transiently transfected with the plasmids pGal5-Tk-pGL3 and pGal4-hPPARγDEF, which enabled to quantify the efficacy of the compounds to activate PPARγ.

Furthermore, PPARγ antagonists were examined as cell death modulators for the first time in order to evaluate the role of PPARγ inactivation in the mechanism of action.

2. Results and discussion

2.1. Synthesis

The syntheses of target compounds (Scheme 1) were performed as published in Refs. [11,14] and the corresponding analytical data coincide with our previous findings. For further details on the preparation of the compounds **1a-g** see Ref. [11].

To synthesize the carbonitriles (**2**), 4'-(bromomethyl)-[1,1′-biphenyl]-2-carbonitrile served as reagent for *N*-alkylation of **1a-g**, whereas methyl 4'-(bromomethyl)-[1,1′-biphenyl]-2-carboxylate was applied to generate the carboxymethyl esters (**3**). These

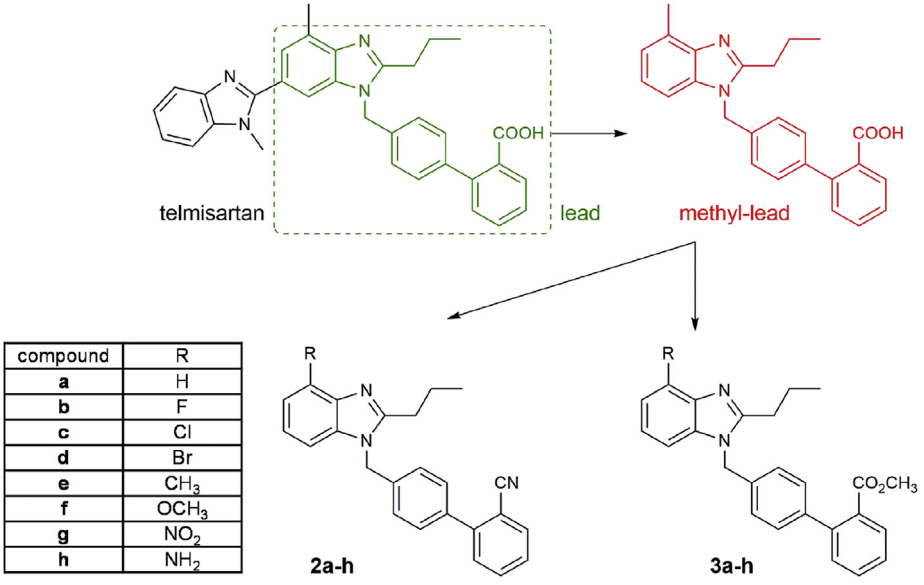

compound	R
a	H
b	F
c	Cl
d	Br
e	CH_3
f	OCH_3
g	NO_2
h	NH_2

Fig. 1. Structures of telmisartan, the lead (colored in green), the methyl-lead (colored in red), and the investigated compounds **2a-h** and **3a-h**.

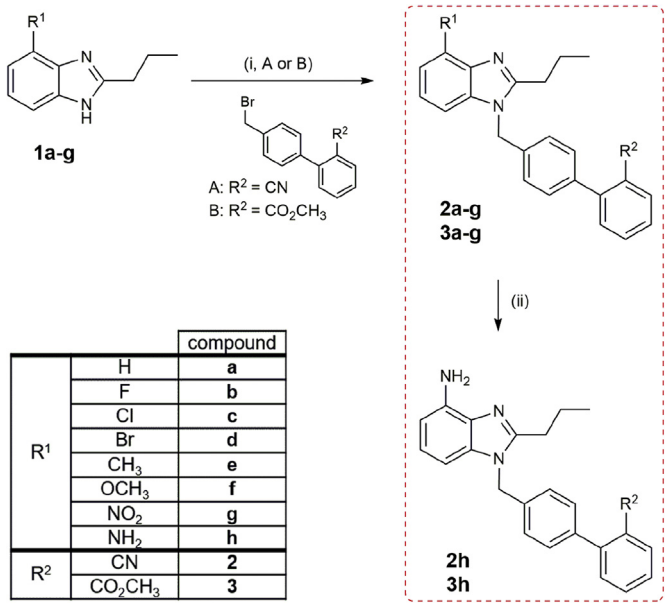

		compound
R^1	H	**a**
	F	**b**
	Cl	**c**
	Br	**d**
	CH_3	**e**
	OCH_3	**f**
	NO_2	**g**
	NH_2	**h**
R^2	CN	**2**
	CO_2CH_3	**3**

Scheme 1. Syntheses of 4'-((4-methyl-2-propyl-1*H*-benzo[*d*]imidazol-1-yl)methyl)-[1,1′-biphenyl]-2-carboxylic acid derivatives. Reagents and conditions: (i) NaH, anhydrous DMF, 0 °C to rt; (ii) H_2, Pd/C, MeOH, rt.

reactions yielded isomeric mixtures of 4- and 7-substituted benzimidazoles, from which **2a-g** and **3a-g** were separated by flash column chromatography. Finally, reduction of **2g** and **3g** with H_2 and Pd/C in MeOH yielded **2h** and **3h**.

^{1}H and ^{13}C NMR spectroscopy as well as high-resolution mass spectrometry (HRMS) indicated the identity of **2a-h** and **3a-h** and HPLC assured a purity of >95%. For detailed information on the analytical data of target compounds see the Supporting Information.

2.2. Biological activity

2.2.1. Induction of cell death and cytotoxicity assays

Pioglitazone and telmisartan, two established drugs in the treatment of diabetes mellitus type II or hypertension, demonstrated potency as sensitizers for chemotherapeutics [8,9,12]. Beside the ability to activate PPARγ, both agents show an effect on STAT5-signalling in resistant K562 cells. Co-application of telmisartan with imatinib (1 μM) reinstated the efficacy of the TKI in this cell line (cell death: 21% (1.75 μM of telmisartan), 57% (5 μM of telmisartan), and 63% (10 μM of telmisartan)). An optimization of this effect was achieved by derivatization of the 2-COOH group at the biphenyl moiety to a 2-$CONH_2$ (cell death: 41% (1.75 μM of telmisartan-amide), 76% (5 μM of telmisartan-amide), and 89% (10 μM of telmisartan-amide)) [12]. These positive results induced us to screen the new series of carbonitrile (**2a-h**) and carboxymethyl ester (**3a-h**) derivatives of the methyl-lead in the same manner.

First of all, the potency to sensitize K562-resistant cells to imatinib treatment was evaluated. Co-application of the compounds **2a-g** or **3a-g** at a concentration of 10 μM increased the cell death rate induced by imatinib (1 μM) from 19% (inactive < 20%, Fig. 2B) to > 85% (data not shown). Therefore, we used a concentration of 5 μM in order to deduce a clear SAR. At this concentration, all compounds were *per se* inactive and did not induce a cell death rate higher than 20%. Most of them caused effects comparable to the vehicle treated control (DMSO, ctr. in Fig. 2A). Yet, the combination with imatinib (1 μM) clearly demonstrated their cell death modulating properties (Fig. 2B).

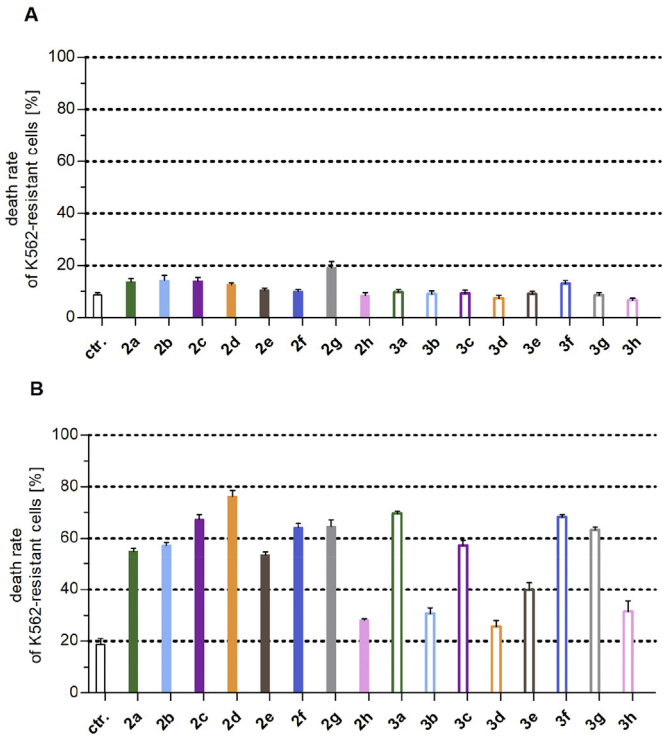

Fig. 2. Results of the PI FACS analyses, investigating the death rate of K562-resistant cells caused by the compounds **2a-h** and **3a-h** (5 μM each) without (A) or combined with 1 μM of imatinib (B). Ctr. (DMSO) conforms to the vehicle treated control without (A) or with imatinib (B). Data represent the mean + SEM of ≥3 independent experiments.

The 2-carbonitriles **2a-g** are highly effective sensitizers and allowed imatinib to cause a cell death rate of 50–80% (Fig. 2B). Most active was the 4-Br derivative **2d**, which enabled imatinib to induce >76% cell death, whereas 4-NH_2 substitution resulted in the less potent compound **2h** (28%). It is worth mentioning that the formerly investigated 2-COOH derivatives were more or less inactive and only marginally increased the efficacy of imatinib. Also compared to the previously described carboxamides, **2a-g** were considerably more potent.

The 2-CO_2CH_3-substituted compounds gave a more differentiated picture. In this series, the substituent at position 4 of the benzimidazole markedly influenced the cell death rate. Compounds **3a** (H), **3c** (Cl), **3f** (OCH_3), and **3g** (NO_2) equally sensitized the cells to imatinib treatment (57–70% cell death, Fig. 2B). Slightly less activity (40% cell death) was observed for **3e** (CH_3). Finally, the compounds **3b** (F), **3d** (Br), and **3h** (NH_2) showed only low sensitizing efficacy at 5 μM (26–32% cell death).

In summary, these outcomes are far better compared to our previous study [11]. Even at the low concentration of 5 μM, which is considered as patient-relevant, the new derivatives enabled imatinib to cause a cell death rate of >76%, while the cell death modulators designed before only enhanced the activity of imatinib up to 31%. As a very important result, we confirmed that the substituent at position 2 of the biphenyl core is essential for the sensitizing effects, which increase in the following order: 2-COOH [11] < 2-$CONH_2$ [11] < 2-CO_2CH_3 < 2-CN. Fine-tuning of the efficacy can be realized by substituents at position 4 of the benzimidazole.

To ensure that these sensitizing effects are not caused by unselective cytotoxicity of the compounds, all derivatives were examined in the non-malignant human bone marrow/stroma cell line HS-5 by PI FACS analyses. Either applied with or without imatinib, **2a-h** and **3a-h** did not induce significant cell death at

5 μM (equal to the concentration within the PI FACS analyses in K562-resistant cells). The compounds *per se* as well as their combination with imatinib can therefore be verified as non-cytotoxic (Fig. 3).

Of further interest was the influence on the viability of non-malignant monkey kidney fibroblast-like COS-7 cells. These cells were used in the transactivation assay to determine PPARγ activation.

Actively growing cells show a high metabolic activity. Accordingly, NAD(P)H-dependent cellular enzymes catalyze the reaction of the used MTT dye, which consists of a tetrazolium salt, to its purple-colored formazan [16]. A high rate of transformation relates to a large quantity of cells with functional mitochondria. Restricted viability has a negative impact on the transactivation and interferes with the determination of the agonistic potency.

None of the tested compounds (**2a-h** and **3a-h**) reduced the cell viability despite the high concentration of 10 μM (Fig. 4). Thus, COS-7 cells could be used to determine the PPARγ activity of the derivatives up to this concentration in the dual-luciferase reporter assay (results are shown in Table 1 and Fig. 5).

To complete our studies on cytotoxicity, PI FACS analyses were also performed with the compounds alone or in combination with imatinib using COS-7 cells (see Supporting Information Figure S49). Again, no alteration of cell death was observed in both cases.

2.2.2. Transactivation assay

As mentioned above, our main aim was to reduce the PPARγ activity of the generated compounds and to efficiently sensitize K562-resistant cells to imatinib at the same time. In order to evaluate the extent of PPARγ agonism, the receptor activation induced by **2a-h** and **3a-h** was quantified in a dual-luciferase reporter assay in COS-7 cells, transiently transfected with the plasmids pGal5-TK-pGL3, pGal4-hPPARγDEF, and pRenilla-CMV.

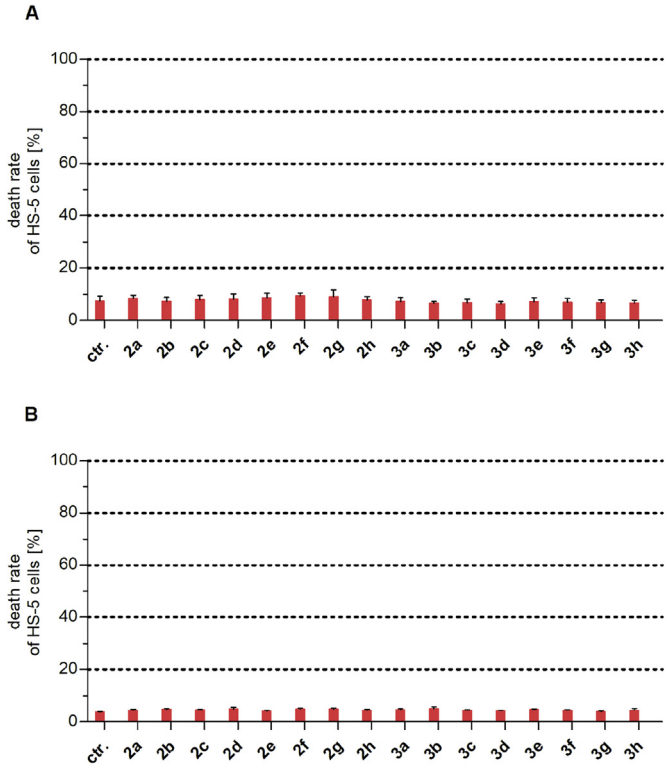

Fig. 3. Death rate of HS-5 cells treated with 5 μM of each of the compounds **2a-h** and **3a-h** either without (A) or combined with 1 μM of imatinib (B). Ctr. (DMSO) represents the vehicle treated control without (A) or with imatinib (B). Depicted are the mean values + SEM of ≥3 independent PI FACS experiments.

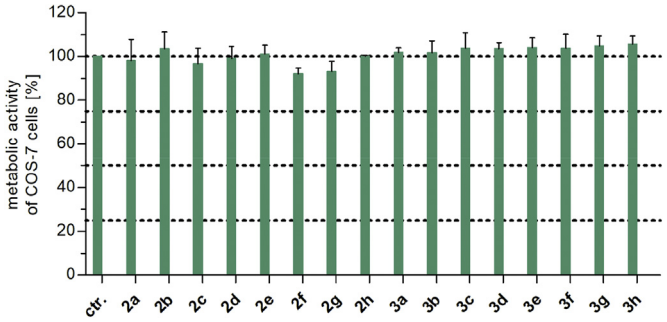

Fig. 4. Results of the modified MTT assay. COS-7 cells were treated with vehicle (DMSO, ctr.), the compounds **2a-h**, and **3a-h** at 10 μM, respectively. Depicted are the mean values + SD of ≥4 independent experiments.

Pioglitazone, which represents a full PPARγ agonist, served as reference and its intrinsic activity at 10 μM was set to 100% (A_{max}). The effects of the compounds or the vehicle-treated control were related to this value (A_{max} [%]). Telmisartan yielded an A_{max} of 59.8%, perfectly matching the literature [11,14]. The results of all tested compounds (at 10 μM) are listed in Table 1 and the concentration-activation curves, comprising the concentrations 0.05–10 μM, are depicted in Fig. 5.

Interestingly, the carbonitriles generally yielded partial intrinsic activity on PPARγ (Table 1), but did not reach the effect of pioglitazone. The most effective compounds **2a** (A_{max} = 64.5%), **2b** (A_{max} = 76.0%), and **2c** (A_{max} = 68.4%), caused concentration-response curves (Fig. 5) comparable to telmisartan (A_{max} = 59.8%). Somewhat weaker agonistic properties were determined for **2d-h** with A_{max} = 32.2%–45.9%. The effects of **2a-e** were similar to that of the related 2-COOH derivatives [11], while **2f-h** showed slightly higher activity.

Derivatization of the carboxylic group to a carboxymethyl ester strongly diminished the interaction with PPARγ. **3a-h** induced an activation of at most 22% at 10 μM. Neither the carbonitriles nor the carboxymethyl esters yielded a concentration-dependent saturation of activation. Therefore, their profile corresponds to that of weak agonists rather than of partial agonists (Fig. 5). Comparison of the results with those of the related carboxamides (A_{max} = 7%–40%) indicates a distinctly stronger prevention of PPARγ activity upon esterification.

In summary, it was proven that regarding PPARγ activation, the moiety at position 2 of the biphenyl rather determines the activity than the substituent at position 4 of the benzimidazole (medium versus weak activity, respectively). Carboxylic acids and carbonitriles represent partial agonists without the option to reach the maximum effect of the full agonist pioglitazone. Esterification and amidation strongly reduced the potency with A_{max} < 30%–40% and corresponding derivatives are therefore beneficial over the carbonitriles. The 4-substitution at the benzimidazole core is of minor importance, as the activity within the groups barely changes.

2.2.3. Analyses of protein expression

It has been demonstrated that pioglitazone reduces the expression of STAT5 and its downstream targets HIF2α and CITED2, which are key guardians of the quiescence and stemness of LSCs, *in vitro*. The positive preclinical results of the combination of imatinib and pioglitazone led to their investigation within the ACTIM phase II clinical trial, where the former findings of STAT5 down-regulation could be confirmed [8,9]. However, the recent EDI-PIO trial revealed that there was no significant difference in STAT5

Table 1
Summarized results of the transactivation assay with COS-7 cells, transiently transfected with the plasmids pGal5-TK-pGL3, pGal4-hPPARγDEF, and pRenilla-CMV.

R	compound	A_{max} [%][a,b] at 10 μM	R	compound	A_{max} [%][a,b] at 10 μM
	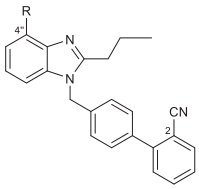			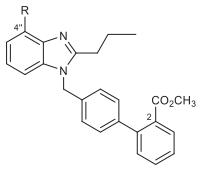	
H	**2a**	64.5 ± 7.4	H	**3a**	21.6 ± 1.3
F	**2b**	76.0 ± 7.3	F	**3b**	14.7 ± 1.1
Cl	**2c**	68.4 ± 8.3	Cl	**3c**	22.2 ± 3.5
Br	**2d**	41.1 ± 3.8	Br	**3d**	11.6 ± 0.8
CH_3	**2e**	32.2 ± 4.3	CH_3	**3e**	13.8 ± 2.7
OCH_3	**2f**	45.9 ± 5.8	OCH_3	**3f**	20.7 ± 4.4
NO_2	**2g**	37.9 ± 4.1	NO_2	**3g**	15.0 ± 1.3
NH_2	**2h**	43.0 ± 6.2	NH_2	**3h**	0.11 ± 0.10
pioglitazone		100			
telmisartan		59.8 ± 4.6			

[a] A_{max} [%] is the intrinsic activity of each compound on PPARγ, related to that of pioglitazone (A_{max} = 100%).
[b] Data represent the mean ± SD of ≥3 independent experiments.

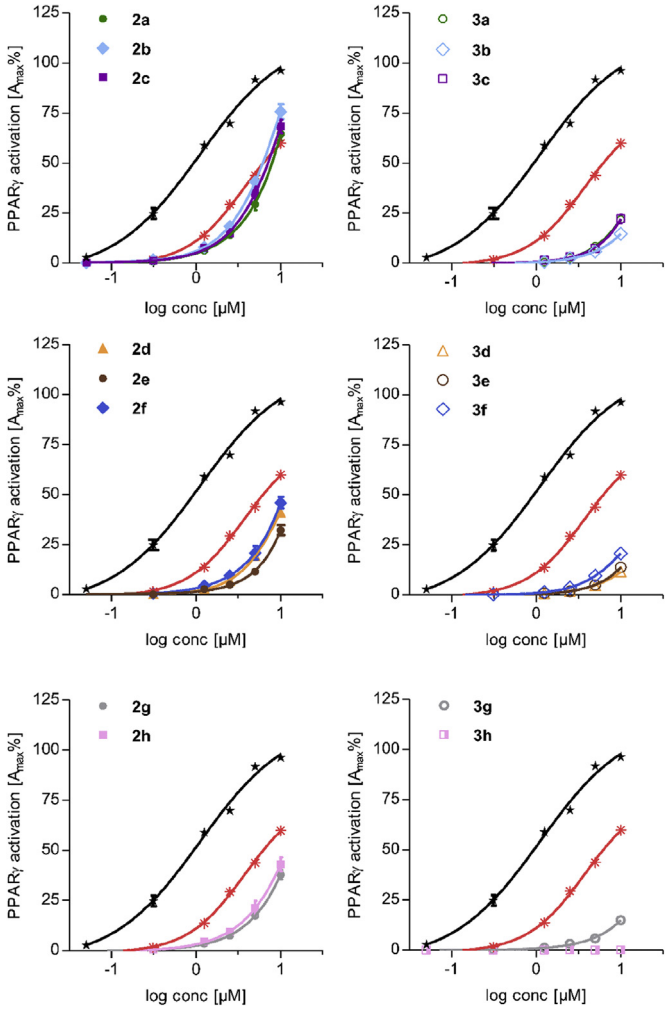

Fig. 5. Concentration-response curves caused by **2a-h** and **3a-h** in the dual-luciferase reporter assay using COS-7 cells transiently transfected with the plasmids pGal5-TKpGL3, pGal4-hPPARγDEF, and pRenilla-CMV. Pioglitazone (★) and telmisartan (✳) were used as references. The data represent the mean ± SD of ≥3 independent experiments with three replicates each.

expression in CML patients treated with imatinib and pioglitazone [17]. Though these results are inconsistent, various studies report the role of STAT5 as critical tumor maintainer and inducer of resistance in hematological malignancies [18,19]. Thus, we investigated STAT5 and its phosphorylation status at tyrosine 694/699 (→ pSTAT5), which is a key marker of STAT5 activation. In BCR-ABL-positive cells, STAT5 is steadily phosphorylated and therefore constitutively activated. In sensitive CML cells, e.g. in K562 CML cells, Jacobberger et al. [20] found the repression of pSTAT5 and the consequent inhibition of STAT5 by imatinib. However, the overexpression of STAT5 in resistant cells or LSCs, mediates imatinib resistance and is associated with disease progression [19].

The impact of **2a-d** and **3a-d** on the expression of STAT5 and pSTAT5 was investigated by the capillary-based Jess Simple Western™ immunoassay (for the complete blots see Supporting Figure S51). For this purpose, K562-resistant cells were treated

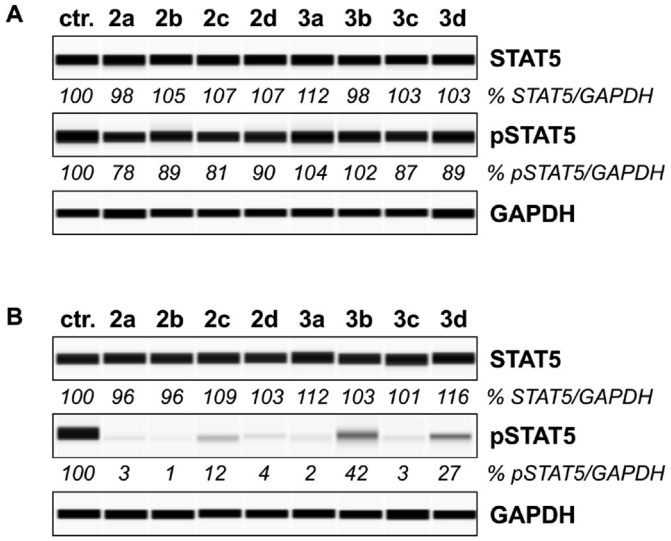

Fig. 6. Jess Simple Western™ immunoassays of STAT5 and pSTAT5 expression in K562-resistant cells treated for 6 h with 5 μM of **2a-d**, **3a-d**, or vehicle (ctr., DMSO) alone (A), and in combination with 1 μM of imatinib (B), respectively. GAPDH served as loading control.

without or with imatinib (1 μM) and the compounds (5 μM) for 6 h. As depicted in Fig. 6, the STAT5 and pSTAT5 expression was not markedly affected by the compounds alone (Fig. 6A) and STAT5 was also not downregulated by combining the compounds with imatinib (Fig. 6B).

In contrast, the combination of imatinib with **2a-d**, **3a**, or **3c** strongly repressed the phosphorylation status of STAT5 (pSTAT5 ↓). In case of **3b** and **3d**, the effect was somewhat less pronounced. The inactivity of imatinib or the compounds when used alone indicates an indirect impact on STAT5 phosphorylation in K562-resistant cells.

This outcome perfectly coincides with the results of the cell death induction (PI FACS analyses, Fig. 2). Although the compounds were *per se* inactive at K562-resistant cells, they sensitized the cells to imatinib treatment. These findings suggest that the repression of STAT5 phosphorylation is part of the mode of action. However, the detailed molecular mechanism has to be investigated in ongoing studies.

2.3. Discussion

In the present study, we continued our investigations on the circumvention of imatinib resistance in leukemia cells. Previously, we developed potent cell death modulators derived from telmisartan and showed that their use as non-cytotoxic add-ons restored imatinib activity in resistant cell lines. This was demonstrated for telmisartan, but also for the 4'-((2-propyl-1*H*-benzo[*d*]imidazol-1-yl)methyl)-[1,1′-biphenyl]-2-carboxylic acid (lead). Derivatization was performed at the 2-COOH group of both and additionally at position 4 of the benzimidazole core based on the 4'-((4-methyl-2-propyl-1*H*-benzo[*d*]imidazol-1-yl)methyl)-[1,1′-biphenyl]-2-carboxylic acid (methyl-lead).

The PI FACS analyses using K562-resistant cells revealed high sensitizing properties for all novel compounds at 10 μM. Despite their non-cytotoxic properties, the derivatives strongly increased the effects of imatinib in resistant leukemia cells. The extent mainly depended on the nature of the substituent at position 2 of the biphenyl moiety. Telmisartan and its 2-carboxamide were much more effective than pioglitazone, which did not even show efficacy at > 10 μM. At 5 μM they mediated a cell death rate of 57% and 76% in combination with imatinib (1 μM), respectively.

Derivatization of the 2-COOH group at the biphenyl moiety of the lead to an amide, and especially to an ester or a carbonitrile considerably increased the sensitizing potency (2-COOH < 2-$CONH_2$ < 2-CO_2CH_3 < 2-CN). Substituents at position 4 of the benzimidazole allowed an effective fine-tuning. At 5 μM, compounds with a 4-H, 4-Cl, 4-OCH_3, and 4-NO_2 substituent showed the highest potency in the ester series (**3**) (>60% cell death induced by imatinib), while 4-Cl, 4-Br, 4-OCH_3, and 4-NO_2 substitution resulted in the most active derivatives of the carbonitriles (**2**).

The attempt to increase the activity of the brominated carboxymethyl ester **3d** (66% at 10 μM) by shifting the Br substituent from position 4 to position 5 (5-Br-CO_2CH_3) or 6 (6-Br-CO_2CH_3) of the benzimidazole failed. Although used at the same concentration as add-ons, only 31% and 63% of cell death was caused together with imatinib, respectively. This finding points to the great importance of position 4.

Analogously to pioglitazone, the activation of PPARγ was postulated as mode of action. However, the correlation between the potency as cell death modulator and the PPARγ activity is contradictory (Fig. 7). While the esters **3a-h** generally cause low receptor activation at 10 μM, they act as strong sensitizers to imatinib treatment at the same concentration. A linear correlation can be supposed.

On the contrary, the carbonitriles induced the intrinsic activity of partial PPARγ agonists. In some cases, they were even equipotent to telmisartan. As depicted in Fig. 7, though, the cell death modulating effects and the receptor activity showed no clear correlation. Therefore, PPARγ activation is not part of the mode of action as a sensitizer in this series of compounds.

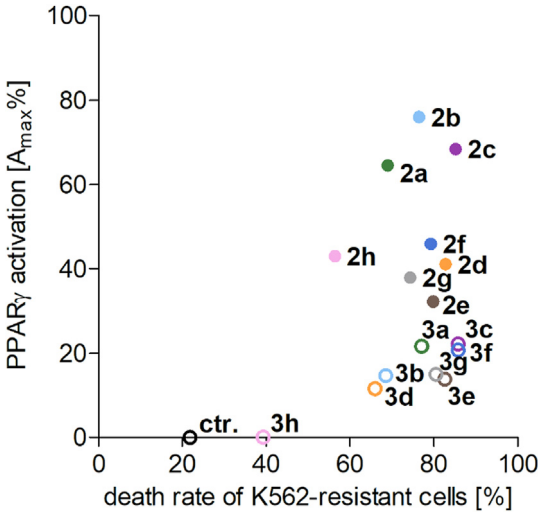

Fig. 7. Correlation between the efficacy of the compounds to activate PPARγ and their potency to sensitize K562-resistant cells to imatinib treatment. Data represent the values of the transactivation assay (A_{max}) and the PI FACS analyses at a concentration of 10 μM.

Since it is well known that partial agonists comprise also the pharmacological profile of antagonists, we included the reversible PPARγ antagonist diclofenac and the irreversible binder GW9662 in this SAR study [21,22]. Both compounds, however, were not able to increase the cytotoxicity of imatinib in K562-resistant cells (see Supporting Figure S50). Consequently, the inhibition of PPARγ does not seem to play an essential role in the mode of action.

Considering all findings, the design and development of novel cell death modulators to treat imatinib resistance should preferably focus on compounds with low PPARγ activity, since no negative impact on the sensitizing activity can be expected (see carboxymethyl ester derivatives). Importantly, typical PPARγ-induced side effects can be prevented in this way.

As the transcription factor STAT5 represents a critical factor for the initiation and maintenance of LSCs, its expression and phosphorylation upon treatment with imatinib was analyzed by immunoassays. Imatinib, telmisartan, and related derivatives including the lead did not influence the STAT5 expression in K562-resistant cells. This was also true when imatinib was administered together with the most active cell death modulators **2a-d** and **3a-d**. Yet, the co-application led to a strong repression of STAT5 phosphorylation, which was not observed when the compounds were administered alone. This outcome indicates that the used derivatives amplified the imatinib-mediated downregulation of pSTAT5, which in turn drives the resistant CML cells into cell death.

3. Conclusions

This study revealed the development of promising novel cell death modulators, which showed improved efficacy in sensitizing K562-resistant cells for imatinib treatment at patient-relevant concentrations. The lead 4'-((2-propyl-1*H*-benzo[*d*]imidazol-1-yl)methyl)-[1,1′-biphenyl]-2-carboxylic acid exhibited high activity, if the 2-carboxylic acid was replaced by a new kind of substituent, the carbonitrile, or a carboxymethyl ester and if hydrophobic substituents were located at position 4 of the benzimidazole core.

Although the derivatives represent analogues of telmisartan and some acted similarly to partial PPARγ agonists, we could demonstrate that the interaction with this receptor plays a minor role. There was no clear correlation between the cell death modulating effects and the PPARγ activation by the compounds or the inactivation by respective antagonists. Hence, novel cell death modulators should preferably exhibit low PPARγ activity, since no negative influence on sensitization is expected and the side effects that are associated with high receptor activation can be reduced. This was illustrated by the example of the carboxymethyl esters (see the results of e.g. **3f**). Furthermore, all sensitizing derivatives strongly repressed the phosphorylation status of STAT5, when combined with imatinib. It is therefore likely that STAT5 is involved in the mechanism of action and that the disruption of this central signaling node has drastic impact on the cell viability of resistant CML cells. Notably, the combination therapy of the new compounds and imatinib induced no cell death in non-malignant cell lines (HS-5 and COS-7), underlining a selective re-sensitization of K562-resistant cells to imatinib treatment. These results are of importance for the further design of non-cytotoxic cell death modulators and may provide valuable information for the development of chemosensitizers for a variety of malignancies.

4. Experimental section

4.1. Chemistry

4.1.1. General materials and methods

All reagents or further chemicals were purchased from Alfa Aesar, Sigma Aldrich, and TCI Chemicals. The compounds **1a-g**, **2a-g**, **3a-c**, and **3e** were synthesized according to Refs. [11,14] and their analytical data are consistent. All solvents were purified before usage by distillation, except ethyl acetate (EA), petroleum ether (PE), and *N,N*-dimethylformamide (DMF), which were purchased in adequate quality. An Isolera One 3.0 flash purification system (Biotage) served to perform medium pressure liquid chromatography, using silica gel 60 (particle size 40–63 μm, 230–240 mesh) as stationary phase. To carry out thin-layer chromatography, Polygram SIL G/UV$_{254}$ polyester foils that were covered with a 0.2 mm layer of silica gel as well as a fluorescence indicator (Macherey-Nagel) were used and visualized with UV light (254 or 366 nm). A 400 MHz Avance 4 Neo (Bruker) and a 700 MHz Avance 4 Neo (Bruker) spectrometer served to record nuclear magnetic resonance spectra (NMR). For this purpose, deuterated dimethyl sulfoxide (DMSO-d_6), acetone (acetone-d_6), and methanol (CD_3OD) were used as solvents (Eurisotop). Chemical shifts (δ) are reported in parts per million (ppm) and were either referred to the solvent peak or tetramethylsilane (TMS) as internal standard. Coupling constants (J) are given in Hertz (Hz). Signals are described as follows: s = singlet, d = doublet, dd = doublet of doublets, t = triplet, m = multiplet. An Orbitrap Elite system (Thermo Fisher Scientific) was applied to implement HRMS. HPLC was further used to determine the purity of the compounds. The Shimadzu Nexera-i LC-2040C-3D device with the autosampler SIL-20A HT, the column oven CTO-10AS VP, the degasser DGU-20A, the detector SPD-M20A, and the pumps LC-20AD was employed. An RP-18 column (dimension 250 × 4 mm, 5 μm particle size, Knauer) served as stationary phase and methanol/water as mobile phase. The chromatograms were analyzed with the program LabSolutions 5.86 (Shimadzu). All compounds exhibited a purity of >95%.

4.1.2. General procedure for the N-alkylation

The dried benzimidazoles **1a-g** (1 eq) were dissolved in anhydrous DMF (~1–2.5 ml/mmol) under an argon atmosphere and it was cooled to 0 °C in an ice bath. After slowly adding NaH (1.2 eq), the mixture was stirred for 30 min on ice. Either 4'-(bromomethyl)-[1,1′-biphenyl]-2-carbonitrile or methyl 4'-(bromomethyl)-[1,1′-biphenyl]-2-carboxylate (1.1 eq each) was added and the reaction mixture was stirred at room temperature for 5–16 h. Then, it was diluted with ice water to double the volume and 1 N HCl was applied for neutralization. The solution was extracted three times with EA and the organic layers were combined, washed with brine, dried over anhydrous Na_2SO_4, and filtered. After removing the solvent under reduced pressure, the crude product was purified by flash column chromatography with stepwise gradient elution (PE/EA, 7:3 to 3:7).

*4.1.2.1. 4'-((2-Propyl-1H-benzo[d]imidazol-1-yl)methyl)-[1,1′-biphenyl]-2-carbonitrile (**2a**).* ^{1}H NMR (400 MHz, acetone-d_6): δ 7.87 (dd, ^3J = 7.7 Hz, ^4J = 0.8 Hz, 1H, *H3*), 7.79-7.72 (m, 1H, *H5*), 7.64-7.53 (m, 5H, *H4*, *H6*, *H2′*, *H6′*, *H4″*), 7.46-7.41 (m, 1H, *H7″*), 7.27 (d, ^3J = 8.5 Hz, 2H, *H3′*, *H5′*), 7.21-7.14 (m, 2H, *H5″*, *H6″*), 5.62 (s, 2H, *NCH$_2$*), 2.90 (t, ^3J = 7.6 Hz, 2H, *CH$_2$*CH$_2$CH$_3$), 1.95-1.81 (m, 2H, CH$_2$*CH$_2$*CH$_3$), 1.01 (t, ^3J = 7.4 Hz, 3H, CH$_2$CH$_2$*CH$_3$*). ^{13}C NMR (101 MHz, acetone-d_6): δ 156.0, 145.4, 144.2, 138.9, 138.5, 136.6, 134.7, 134.1, 131.0, 130.8, 130.1, 129.9, 129.0, 127.6, 122.7, 122.3, 119.8, 119.1, 111.9, 110.7, 46.9, 21.5, 14.2. HRMS: *m/z* calculated for $C_{24}H_{21}N_3$ $[M+H]^+$: 352.1808, found: 352.1810.

*4.1.2.2. 4'-((4-Fluoro-2-propyl-1H-benzo[d]imidazol-1-yl)methyl)-[1,1′-biphenyl]-2-carbonitrile (**2b**).* ^{1}H NMR (400 MHz, acetone-d_6): δ 7.87 (dd, ^3J = 7.6 Hz, ^4J = 0.8 Hz, 1H, *H3*), 7.80-7.74 (m, 1H, *H5*), 7.63-7.55 (m, 4H, *H4*, *H6*, *H2′*, *H6′*), 7.32-7.26 (m, 3H, *H3′*, *H5′*, *H7″*), 7.20-7.12 (m, 1H, *H6″*), 6.98-6.89 (m, 1H, *H5″*), 5.65 (s, 2H, *NCH$_2$*), 2.92 (t, ^3J = 7.6 Hz, 2H, *CH$_2$*CH$_2$CH$_3$), 1.96-1.83 (m, 2H, CH$_2$*CH$_2$*CH$_3$), 1.02 (t, ^3J = 7.4 Hz, 3H, CH$_2$CH$_2$*CH$_3$*). ^{13}C NMR (101 MHz, acetone-d_6): δ 156.7, 155.8, 153.3, 145.4, 139.9, 138.7, 138.5, 134.7, 134.1, 132.3, 131.1, 130.2, 129.0, 127.7, 123.2, 119.1, 112.0, 107.9, 107.7, 107.2, 47.3, 21.4, 14.2. HRMS: *m/z* calculated for $C_{24}H_{20}FN_3$ $[M+H]^+$: 370.1714, found: 370.1721.

*4.1.2.3. 4'-((4-Chloro-2-propyl-1H-benzo[d]imidazol-1-yl)methyl)-[1,1′-biphenyl]-2-carbonitrile (**2c**).* ^{1}H NMR (400 MHz, acetone-d_6): δ 7.87 (dd, ^3J = 8.0 Hz, ^4J = 0.8 Hz, 1H, *H3*), 7.80-7.73 (m, 1H, *H5*), 7.63-7.53 (m, 4H, *H4*, *H6*, *H2′*, *H6′*), 7.43 (dd, ^3J = 8.0 Hz, ^4J = 1.0 Hz, 1H, *H7″*), 7.28 (d, ^3J = 8.4 Hz, 2H, *H3′*, *H5′*), 7.24 (dd, ^3J = 7.8 Hz, ^4J = 1.0 Hz, 1H, *H5″*), 7.19-7.13 (m, 1H, *H6″*), 5.66 (s, 2H, *NCH$_2$*), 2.93 (t, ^3J = 7.6 Hz, 2H, *CH$_2$*CH$_2$CH$_3$), 1.96-1.82 (m, 2H, CH$_2$*CH$_2$*CH$_3$), 1.02 (t, ^3J = 7.4 Hz, 3H, CH$_2$CH$_2$*CH$_3$*). ^{13}C NMR (101 MHz, acetone-d_6): δ 157.2, 145.4, 141.1, 138.7, 138.4, 137.8, 134.7, 134.1, 131.0, 130.2, 129.0, 127.7, 124.4, 123.4, 122.4, 119.1, 112.0, 109.9, 47.3, 21.5, 14.2. HRMS: *m/z* calculated for $C_{24}H_{20}ClN_3$ $[M+H]^+$: 386.1419, found: 386.1429.

*4.1.2.4. 4'-((4-Bromo-2-propyl-1H-benzo[d]imidazol-1-yl)methyl)-[1,1′-biphenyl]-2-carbonitrile (**2d**).* ^{1}H NMR (400 MHz, acetone-d_6): δ 7.87 (dd, ^3J = 7.7 Hz, ^4J = 0.8 Hz, 1H, *H3*), 7.80-7.73 (m, 1H, *H5*), 7.62-7.55 (m, 4H, *H4*, *H6*, *H2′*, *H6′*), 7.47 (dd, ^3J = 8.0 Hz, ^4J = 0.9 Hz, 1H, *H7″*), 7.41 (dd, ^3J = 7.8 Hz, ^4J = 0.9 Hz, 1H, *H5″*), 7.28 (d, ^3J = 8.6 Hz, 2H, *H3′*, *H5′*), 7.14-7.08 (m, 1H, *H6″*), 5.65 (s, 2H, *NCH$_2$*), 2.93 (t, ^3J = 7.6 Hz, 2H, *CH$_2$*CH$_2$CH$_3$), 1.94-1.82 (m, 2H, CH$_2$*CH$_2$*CH$_3$), 1.02 (t, ^3J = 7.4 Hz, 3H, CH$_2$CH$_2$*CH$_3$*). ^{13}C NMR (101 MHz, acetone-d_6): δ 157.1, 145.4, 142.5, 138.7, 138.4, 137.3, 134.7, 134.1, 131.0, 130.2, 129.0, 127.7, 125.5, 123.8, 119.1, 113.2, 112.0, 110.4, 47.4, 21.6, 14.2. HRMS: *m/z* calculated for $C_{24}H_{20}BrN_3$ $[M+H]^+$: 430.0913, found: 430.0931.

*4.1.2.5. 4'-((4-Methyl-2-propyl-1H-benzo[d]imidazol-1-yl)methyl)-[1,1′-biphenyl]-2-carbonitrile (**2e**).* ^{1}H NMR (400 MHz, acetone-d_6): δ 7.87 (dd, ^3J = 7.7 Hz, ^4J = 0.8 Hz, 1H, *H3*), 7.80-7.72 (m, 1H, *H5*),

7.61-7.54 (m, 4H, *H4*, *H6*, *H2′*, *H6′*), 7.29-7.22 (m, 3H, *H3′*, *H5′*, *H7‴*), 7.09-7.03 (m, 1H, *H6″*), 6.99 (d, ^3J = 7.3 Hz, 1H, *H5″*), 5.59 (s, 2H, *NCH*$_2$), 2.89 (t, ^3J = 7.6 Hz, 2H, *CH*$_2$CH$_2$CH$_3$), 2.59 (s, 3H, *CH*$_3$), 1.94-1.80 (m, 2H, CH$_2$*CH*$_2$CH$_3$), 1.02 (t, ^3J = 7.4 Hz, 3H, CH$_2$CH$_2$*CH*$_3$). ^{13}C NMR (101 MHz, acetone-d_6): δ 155.1, 145.5, 143.3, 139.0, 138.5, 136.2, 134.7, 134.1, 131.0, 130.1, 129.5, 129.0, 127.6, 122.7, 122.6, 119.1, 111.9, 108.2, 47.0, 21.8, 16.7, 14.3. HRMS: *m/z* calculated for $C_{25}H_{23}N_3$ $[M+H]^+$: 366.1965, found: 366.1977.

*4.1.2.6. 4′-((4-Methoxy-2-propyl-1H-benzo[d]imidazol-1-yl)methyl)-[1,1′-biphenyl]-2-carbonitrile (**2f**).* ^{1}H NMR (400 MHz, acetone-d_6): δ 7.87 (dd, ^3J = 7.7 Hz, ^4J = 1.2 Hz, 1H, *H3*), 7.79-7.73 (m, 1H, *H5*), 7.62-7.53 (m, 4H, *H4*, *H6*, *H2′*, *H6′*), 7.26 (d, ^3J = 8.6 Hz, 2H, *H3′*, *H5′*), 7.12-7.00 (m, 2H, *H6″*, *H7‴*), 6.70 (dd, ^3J = 7.8 Hz, ^4J = 1.0 Hz, 1H, *H5″*), 5.58 (s, 2H, *NCH*$_2$), 4.02 (s, 3H, *OCH*$_3$), 2.87 (t, ^3J = 7.4 Hz, 2H, *CH*$_2$CH$_2$CH$_3$), 1.93-1.81 (m, 2H, CH$_2$*CH*$_2$CH$_3$), 1.01 (t, ^3J = 7.4 Hz, 3H, CH$_2$CH$_2$*CH*$_3$). ^{13}C NMR (101 MHz, acetone-d_6): δ 154.3, 152.3, 145.4, 138.9, 138.5, 134.7, 134.1, 131.0, 130.1, 129.0, 127.6, 123.5, 119.1, 111.9, 104.6, 103.7, 56.4, 47.0, 21.5, 14.2. HRMS: *m/z* calculated for $C_{25}H_{23}N_3O$ $[M+H]^+$: 382.1914, found: 382.1930.

*4.1.2.7. 4′-((4-Nitro-2-propyl-1H-benzo[d]imidazol-1-yl)methyl)-[1,1′-biphenyl]-2-carbonitrile (**2g**).* ^{1}H NMR (400 MHz, acetone-d_6): δ 8.01 (dd, ^3J = 8.0 Hz, ^4J = 0.9 Hz, 1H, *H3*), 7.93-7.85 (m, 2H, *H5*, *H5″*), 7.80-7.73 (m, 1H, *H4*), 7.63-7.55 (m, 4H, *H6*, *H2′*, *H6′*, *H7‴*), 7.41-7.35 (m, 1H, *H6″*), 7.31 (d, ^3J = 8.3 Hz, 2H, *H3′*, *H5′*), 5.77 (s, 2H, *NCH*$_2$), 3.01 (t, ^3J = 7.6 Hz, 2H, *CH*$_2$CH$_2$CH$_3$), 1.97-1.83 (m, 2H, CH$_2$*CH*$_2$CH$_3$), 1.03 (t, ^3J = 7.4 Hz, 3H, CH$_2$CH$_2$*CH*$_3$). ^{13}C NMR (101 MHz, acetone-d_6): δ 160.4, 145.3, 139.9, 139.5, 138.9, 138.0, 137.4, 134.7, 134.1, 131.0, 130.3, 129.1, 127.7, 122.0, 119.0, 118.9, 117.1, 111.9, 47.4, 21.6, 14.2. HRMS: *m/z* calculated for $C_{24}H_{20}N_4O_2$ $[M+H]^+$: 397.1659, found: 397.1678.

*4.1.2.8. Methyl 4′-((2-propyl-1H-benzo[d]imidazol-1-yl)methyl)-[1,1′-biphenyl]-2-carboxylate (**3a**).* ^{1}H NMR (400 MHz, DMSO-d_6): δ 7.72 (dd, ^3J = 7.7 Hz, ^4J = 1.2 Hz, 1H, *H3*), 7.63-7.56 (m, 2H, *H5*, *H4‘‘*), 7.52-7.44 (m, 2H, *H4*, *H7‘‘*), 7.38 (dd, ^3J = 7.7 Hz, ^4J = 0.9 Hz, 1H, *H6*), 7.24 (d, ^3J = 8.2 Hz, 2H, *H2‘*, *H6‘*), 7.20-7.11 (m, 4H, *H3‘*, *H5‘*, *H5‘‘*, *H6‘‘*), 5.54 (s, 2H, *NCH*$_2$), 3.54 (s, 3H, *CO*$_2$*CH*$_3$), 2.84 (t, ^3J = 7.5 Hz, 2H, *CH*$_2$CH$_2$CH$_3$), 1.85-1.71 (m, 2H, CH$_2$*CH*$_2$CH$_3$), 0.96 (t, ^3J = 7.4 Hz, 3H, CH$_2$CH$_2$*CH*$_3$). ^{13}C NMR (101 MHz, DMSO-d_6): δ 168.4, 155.1, 142.4, 140.7, 139.7, 136.2, 135.4, 131.5, 130.7, 130.5, 129.3, 128.5, 127.5, 126.4, 121.7, 121.3, 118.5, 110.1, 51.8, 45.7, 28.6, 20.3, 13.8. HRMS: *m/z* calculated for $C_{25}H_{24}N_2O_2$ $[M+H]^+$: 385.1911, found: 385.1934.

*4.1.2.9. Methyl 4′-((4-fluoro-2-propyl-1H-benzo[d]imidazol-1-yl) methyl)-[1,1′-biphenyl]-2-carboxylate (**3b**).* ^{1}H NMR (400 MHz, acetone-d_6): δ 7.77 (dd, ^3J = 7.7 Hz, ^4J = 1.1 Hz, 1H, *H3*), 7.62-7.56 (m, 1H, *H5*), 7.49-7.44 (m, 1H, *H4*), 7.40 (dd, ^3J = 7.7 Hz, ^4J = 0.9 Hz, 1H, *H6*), 7.31-7.26 (m, 3H, *H2‘*, *H6‘*, *H7‘‘*), 7.21-7.12 (m, 3H, *H3‘*, *H5‘*, *H6‘‘*), 6.96-6.89 (m, 1H, *H5‘‘*), 5.59 (s, 2H, *NCH*$_2$), 3.56 (s, 3H, *CO*$_2$*CH*$_3$), 2.91 (t, ^3J = 7.6 Hz, 2H, *CH*$_2$CH$_2$CH$_3$), 1.93-1.82 (m, 2H, CH$_2$*CH*$_2$CH$_3$), 1.02 (t, ^3J = 7.4 Hz, 3H, CH$_2$CH$_2$*CH*$_3$). ^{13}C NMR (101 MHz, acetone-d_6): δ 169.3, 156.7, 142.4, 141.6, 136.8, 132.3, 132.2, 131.4, 130.4, 129.7, 128.3, 127.2, 123.2, 123.1, 107.8, 107.7, 107.2, 107.2, 52.1, 47.4, 21.4, 14.2. HRMS: *m/z* calculated for $C_{25}H_{23}FN_2O_2$ $[M+H]^+$: 403.1816, found: 403.1845.

*4.1.2.10. Methyl 4′-((4-chloro-2-propyl-1H-benzo[d]imidazol-1-yl) methyl)-[1,1′-biphenyl]-2-carboxylate (**3c**).* ^{1}H NMR (400 MHz, acetone-d_6): δ 7.77 (dd, ^3J = 7.7 Hz, ^4J = 1.1 Hz, 1H, *H3*), 7.62-7.56 (m, 1H, *H5*), 7.50-7.44 (m, 1H, *H4*), 7.43-7.38 (m, 2H, *H6*, *H7‘‘*), 7.29 (d, ^3J = 8.3 Hz, 2H, *H2‘*, *H6‘*), 7.25-7.13 (m, 4H, *H3‘*, *H5‘*, *H5‘‘*, *H6‘‘*), 5.60 (s, 2H, *NCH*$_2$), 3.56 (s, 3H, *CO*$_2$*CH*$_3$), 2.92 (t, ^3J = 7.6 Hz, 2H, *CH*$_2$CH$_2$CH$_3$), 1.94-1.81 (m, 2H, CH$_2$*CH*$_2$CH$_3$), 1.02 (t, ^3J = 7.4 Hz, 3H, CH$_2$CH$_2$*CH*$_3$). ^{13}C NMR (101 MHz, acetone-d_6): δ 169.3, 157.2, 142.3, 141.6, 141.1, 137.9, 136.8, 132.3, 132.2, 131.4, 130.4, 129.7, 128.3, 127.2, 124.4, 123.3, 122.3, 109.9, 52.1, 47.5, 21.5, 14.2. HRMS: *m/z* calculated for $C_{25}H_{23}ClN_2O_2$ $[M+H]^+$: 419.1521, found: 419.1555.

*4.1.2.11. Methyl 4′-((4-bromo-2-propyl-1H-benzo[d]imidazol-1-yl) methyl)-[1,1′-biphenyl]-2-carboxylate (**3d**).* From **1d** (0.10 g 0.4 mmol) in anhydrous DMF (1 ml), with NaH (0.01 g, 0.5 mmol) and methyl 4′-(bromomethyl)-[1,1′-biphenyl]-2-carboxylate (0.14 g, 0.5 mmol). Colorless solid, yield: 38%. ^{1}H NMR (700 MHz, CD$_3$OD): δ 7.78 (dd, ^3J = 7.7 Hz, ^4J = 1.4 Hz, 1H, *H3*), 7.67 (d, ^3J = 7.8 Hz, 1H, *H7‘‘*), 7.63 (d, ^3J = 8.3 Hz, 1H, *H5‘‘*), 7.59-7.54 (m, 1H, *H5*), 7.48-7.43 (m, 1H, *H4*), 7.39-7.33 (m, 2H, *H6*, *H6‘‘*), 7.30 (d, ^3J = 8.3 Hz, 2H, *H2‘*, *H6‘*), 7.24 (d, ^3J = 8.1 Hz, 2H, *H3‘*, *H5‘*), 5.73 (s, 2H, *NCH*$_2$), 3.59 (s, 3H, *CO*$_2$*CH*$_3$), 3.16 (t, ^3J = 7.7 Hz, 2H, *CH*$_2$CH$_2$CH$_3$), 1.85-1.78 (m, 2H, CH$_2$*CH*$_2$CH$_3$), 1.05 (t, ^3J = 7.4 Hz, 3H, CH$_2$CH$_2$*CH*$_3$). ^{13}C NMR (176 MHz, CD$_3$OD): δ 170.5, 163.1, 157.7, 142.9, 135.7, 135.1, 132.6, 132.2, 131.7, 130.8, 130.3, 129.1, 128.7, 127.6, 127.0, 112.6, 52.4, 29.1, 22.6, 14.1. HRMS: *m/z* calculated for $C_{25}H_{23}BrN_2O_2$ $[M+H]^+$: 463.1016, found: 463.1057.

*4.1.2.12. Methyl 4′-((4-methyl-2-propyl-1H-benzo[d]imidazol-1-yl) methyl)-[1,1′-biphenyl]-2-carboxylate (**3e**).* ^{1}H NMR (400 MHz, acetone-d_6): δ 7.76 (dd, ^3J = 7.7 Hz, ^4J = 1.4 Hz, 1H, *H3*), 7.61-7.55 (m, 1H, *H5*), 7.50-7.43 (m, 1H, *H4*), 7.39 (dd, ^3J = 7.9 Hz, ^4J = 1.4 Hz, 1H, *H6*), 7.27 (d, ^3J = 8.3 Hz, 2H, *H2‘*, *H6‘*), 7.22 (d, ^3J = 7.7 Hz, 1H, *H7‘‘*), 7.16 (d, ^3J = 8.5 Hz, 2H, *H3‘*, *H5‘*), 7.08-7.02 (m, 1H, *H6‘‘*), 6.98 (d, ^3J = 7.2 Hz, 1H, *H5‘‘*), 5.53 (s, 2H, *NCH*$_2$), 3.56 (s, 3H, *CO*$_2$*CH*$_3$), 2.88 (t, ^3J = 7.6 Hz, 2H, *CH*$_2$CH$_2$CH$_3$), 2.59 (s, 3H, *CH*$_3$), 1.93-1.79 (m, 2H, CH$_2$*CH*$_2$CH$_3$), 1.02 (t, ^3J = 7.4 Hz, 3H, CH$_2$CH$_2$*CH*$_3$). ^{13}C NMR (101 MHz, acetone-d_6): δ 169.3, 155.1, 143.3, 142.4, 141.4, 137.3, 136.3, 132.3, 132.1, 131.4, 130.4, 129.6, 129.5, 128.2, 127.1, 122.6, 122.5, 108.2, 52.1, 47.1, 21.7, 16.7, 14.3. HRMS: *m/z* calculated for $C_{26}H_{26}N_2O_2$ $[M+H]^+$: 399.2067, found: 399.2104.

*4.1.2.13. Methyl 4′-((4-methoxy-2-propyl-1H-benzo[d]imidazol-1-yl) methyl)-[1,1′-biphenyl]-2-carboxylate (**3f**).* From **1f** (0.70 g, 3.7 mmol) in anhydrous DMF (3 ml), with NaH (0.11 g, 4.4 mmol) and methyl 4′-(bromomethyl)-[1,1′-biphenyl]-2-carboxylate (1.24 g, 4.0 mmol). Colorless solid, yield: 34%. ^{1}H NMR (400 MHz, acetone-d_6): δ 7.76 (dd, ^3J = 7.7 Hz, ^4J = 1.4 Hz, 1H, *H3*), 7.62-7.55 (m, 1H, *H5*), 7.50-7.43 (m, 1H, *H4*), 7.40 (dd, ^3J = 7.5 Hz, ^4J = 1.4 Hz, 1H, *H6*), 7.27 (d, ^3J = 8.3 Hz, 2H, *H2‘*, *H6‘*), 7.16 (d, ^3J = 8.5 Hz, 2H, *H3‘*, *H5‘*), 7.11-7.05 (m, 1H, *H6‘‘*), 7.01 (dd, ^3J = 8.1 Hz, ^4J = 1.0 Hz, 1H, *H7‘‘*), 6.69 (dd, ^3J = 7.8 Hz, ^4J = 0.9 Hz, 1H, H5*‘‘*), 5.53 (s, 2H, *NCH*$_2$), 4.01 (s, 3H, *OCH*$_3$), 3.56 (s, 3H, *CO*$_2$*CH*$_3$), 2.86 (t, ^3J = 7.4 Hz, 2H, *CH*$_2$CH$_2$CH$_3$), 1.92-1.80 (m, 2H, CH$_2$*CH*$_2$CH$_3$), 1.01 (t, ^3J = 7.4 Hz, 3H, CH$_2$CH$_2$*CH*$_3$). ^{13}C NMR (101 MHz, acetone-d_6): δ 169.4, 154.3, 152.3, 142.4, 141.4, 138.5, 137.3, 134.1, 132.3, 132.1, 131.4, 130.4, 129.6, 128.2, 127.1, 123.4, 104.6, 103.7, 56.4, 52.1, 47.1, 21.5, 14.3. HRMS: *m/z* calculated for $C_{26}H_{26}N_2O_3$ $[M+H]^+$: 415.2016, found: 415.2056.

*4.1.2.14. Methyl 4′-((4-nitro-2-propyl-1H-benzo[d]imidazol-1-yl) methyl)-[1,1′-biphenyl]-2-carboxylate (**3g**).* From **1g** (0.80 g, 3.9 mmol) in anhydrous DMF (3 ml), with NaH (0.11 g, 4.7 mmol) and methyl 4′-(bromomethyl)-[1,1′-biphenyl]-2-carboxylate (1.31 g, 4.3 mmol). Colorless solid, yield: 20%. ^{1}H NMR (400 MHz, acetone-d_6): δ 8.00 (dd, ^3J = 8.0 Hz, ^4J = 0.9 Hz, 1H, *H5″*), 7.89 (dd, ^3J = 8.1 Hz, ^4J = 0.9 Hz, 1H, *H7‴*), 7.77 (dd, ^3J = 7.5 Hz, ^4J = 1.2 Hz, 1H, *H3*), 7.62-7.56 (m, 1H, *H5*), 7.50-7.44 (m, 1H, *H4*), 7.42-7.35 (m, 2H, *H6*, *H6″*), 7.30 (d, ^3J = 8.3 Hz, 2H, *H2′*, *H6′*), 7.21 (d, ^3J = 8.5 Hz, 2H, *H3′*, *H5′*), 5.71 (s, 2H, *NCH*$_2$), 3.57 (s, 3H, *CO*$_2$*CH*$_3$), 3.00 (t, ^3J = 7.6 Hz, 2H, *CH*$_2$CH$_2$CH$_3$), 1.95-1.83 (m, 2H, CH$_2$*CH*$_2$CH$_3$), 1.03 (t, *J* = 7.4 Hz, 3H, CH$_2$CH$_2$*CH*$_3$). ^{13}C NMR (101 MHz, acetone-d_6): δ 169.3, 160.4, 142.3, 141.8, 139.9, 139.5, 137.4, 136.3, 132.2, 131.4, 130.5, 129.8, 128.3, 127.2, 121.9, 118.9, 117.2, 52.1, 47.6, 21.6, 14.2. HRMS: *m/z*

calculated for $C_{25}H_{23}N_3O_4$ $[M+H]^+$: 430.1761, found: 430.1806.

4.1.3. General procedure for reduction of the nitro-group

The respective nitro derivative was dissolved in MeOH (200–300 ml/mmol) and Pd/C (0.1 eq) was added carefully under the flow of argon. The suspension was shaken under a hydrogen atmosphere for 2 h. Then, it was filtered and the transparent solution was evaporated.

*4.1.3.1. 4'-((4-Amino-2-propyl-1H-benzo[d]imidazol-1-yl)methyl)-[1,1'-biphenyl]-2-carbonitrile (**2h**).* From **2g** (0.06 g, 0.15 mmol) in MeOH (20 ml) with 10% Pd/C (0.02 g, 0.02 mmol). Colorless solid, yield: 87%. ^{1}H NMR (400 MHz, CD_3OD): δ 7.78 (dd, ^3J = 7.7 Hz, ^4J = 1.1 Hz, 1H, *H3*), 7.70-7.64 (m, 1H, *H5*), 7.52-7.44 (m, 4H, *H4*, *H6*, *H2'*, *H6'*), 7.17 (d, ^3J = 8.6 Hz, 2H, *H3'*, *H5'*), 7.01-6.94 (m, 1H, *H6''*), 6.68 (dd, ^3J = 8.1 Hz, ^4J = 0.9 Hz, 1H, *H7''*), 6.55 (dd, ^3J = 7.7 Hz, ^4J = 0.9 Hz, 1H, *H5''*), 5.44 (s, 2H, *NCH$_2$*), 2.84 (t, ^3J = 7.8 Hz, 2H, *CH$_2$*CH$_2$CH$_3$), 1.84-1.71 (m, 2H, CH$_2$*CH$_2$*CH$_3$), 0.98 (t, ^3J = 7.4 Hz, 3H, CH$_2$CH$_2$*CH$_3$*). ^{13}C NMR (101 MHz, CD_3OD): δ 154.5, 146.1, 139.6, 139.1, 138.9, 137.4, 134.8, 134.4, 131.9, 131.2, 130.4, 129.1, 127.8, 124.9, 119.5, 112.1, 108.1, 100.7, 47.5, 30.1, 22.4, 14.2. HRMS: *m/z* calculated for $C_{24}H_{22}N_4$ $[M+H]^+$: 367.1917, found: 367.1936.

*4.1.3.2. Methyl 4'-((4-amino-2-propyl-1H-benzo[d]imidazol-1-yl) methyl)-[1,1'-biphenyl]-2-carboxylate (**3h**).* From **3g** (0.10 g, 0.23 mmol) in MeOH (30 ml) with 10% Pd/C (0.02 g, 0.02 mmol). Colorless solid, yield: 89%. ^{1}H NMR (400 MHz, CD_3OD): δ 7.73 (dd, ^3J = 7.7 Hz, ^4J = 1.4 Hz, 1H, *H3*), 7.56-7.48 (m, 1H, *H5*), 7.44-7.37 (m, 1H, *H4*), 7.32 (dd, ^3J = 7.7 Hz, ^4J = 0.9 Hz, 1H, *H6*), 7.20 (d, ^3J = 8.2 Hz, 2H, *H2'*, *H6'*), 7.09 (d, ^3J = 8.2 Hz, 2H, *H3'*, *H5'*), 7.02-6.94 (m, 1H, *H6''*), 6.69 (dd, ^3J = 8.1 Hz, ^4J = 0.9 Hz, 1H, *H7''*), 6.55 (dd, ^3J = 7.8 Hz, ^4J = 0.9 Hz, 1H, *H5''*), 5.42 (s, 2H, *NCH$_2$*), 3.55 (s, 3H, *CO$_2$CH$_3$*), 2.86 (t, ^3J = 7.6 Hz, 2H, *CH$_2$*CH$_2$CH$_3$), 1.84-1.72 (m, 2H, CH$_2$*CH$_2$*CH$_3$), 0.99 (t, ^3J = 7.4 Hz, 3H, CH$_2$CH$_2$*CH$_3$*). ^{13}C NMR (101 MHz, CD_3OD): δ 170.7, 154.5, 143.0, 142.1, 139.5, 137.4, 137.2, 132.5, 132.3, 131.7, 130.7, 129.9, 128.4, 127.3, 124.9, 108.1, 100.8, 52.4, 47.6, 30.1, 22.4, 14.2. HRMS: *m/z* calculated for $C_{25}H_{25}N_3O_2$ $[M+H]^+$: 400.2020, found: 400.2064.

4.2. Biology

4.2.1. General cell culture methods

Incubation of the cells was performed in a humidified atmosphere (5% CO_2/95% air) at 37 °C. They were passaged twice per week. Vehicle-treated controls were included within all cell-based assays and the final concentration of DMSO never exceeded 0.1%.

The cultivation of the human bone marrow stromal cell line HS-5 (ATCC) was implemented using Dulbecco's Modified Eagle Medium (DMEM) supplemented with 10% fetal calf serum (FCS, Sigma-Aldrich), 2 mM L-glutamine (GE Healthcare), 100 U/ml penicillin (Lonza), and 100 μg/ml streptomycin (Lonza). The monkey kidney-derived cell line COS-7 (ATCC) was cultured equally, however, without antibiotics, phenol red, or sodium pyruvate. Both cell lines were kept as a monolayer culture.

For the chronic myelogenous leukemia cell lines K562 (ATCC) and K562-resistant, the Roswell Park Memorial Institute (RPMI) 1640 medium (Lonza) supplemented with 10% FCS, 2 mM L-glutamine, 100 U/ml penicillin, and 100 μg/ml streptomycin was used. We received the K562-resistant cells, which were originally described as doxorubicin-resistant subclone of the K562 cell line (termed as KD225 cells) [23], from Ernesto Yague.

4.2.2. Determination of cell death by flow cytometry

Either 2×10^5 K562 cells, 2×10^5 K562-resistant cells, or 0.5×10^5 HS-5 cells per well were seeded in 24-well plates as described previously [11,24]. The compounds were added at the respective concentrations and the cells were incubated for 72 h. Subsequently, the cells were harvested and stained with PI/Triton-X100 for 2 h at 4 °C. Forward/sideward scatter analyses were performed using a CytomicsFC-500 Beckman Coulter. Dead cells were detected as stained nuclei in the sub-G1 marker window. The results of **2a-h** and **3a-h** are represented by the mean ± SEM of ≥3 independent experiments.

4.2.3. Determination of metabolic activity

The metabolic activity was evaluated by a modified MTT colorimetric assay (EZ4U kit, Biomedica). 2×10^3 COS-7 cells per well were seeded in 96-well plates in triplicates and incubated for 24 h. The compounds **2a-h** and **3a-h** were added to obtain a final concentration of 10 μM. After an incubation for 72 h, the appropriate substrate was added. According to the manufacturer's instructions, absorbance was measured and unspecific staining was excluded. To analyze the data, metabolic activity of the control (ctr., DMSO) was set to 100% as reference. The results of the compounds **2a-h** and **3a-h** are represented by the mean + SD of ≥3 independent experiments with threefold determination [25].

4.2.4. Immunoassay

After preparing total protein extracts [12], protein expression was assessed with the capillary-based Jess Simple Western™ detection system (ProteinSimple, Bio-Techne). The assay was performed according to the manufacturer's instructions at default settings. Antibodies specific to STAT5 (#AF2168, R&D Systems; 10 μg/ml) or GAPDH (#2118, Cell Signaling; 0.4 μg/ml) in combination with 0.2 mg/ml protein lysate, the pSTAT5 antibody (#05–886R, Merck; 20 μg/ml) combined with 2 mg/ml protein lysate, as well as the HRP-conjugated secondary anti-rabbit antibody included in the Jess Detection Module kit were used. Data analyses were performed with the Compass for Simple Western™ 4.0 software (ProteinSimple, Bio-Techne).

4.2.5. Dual-luciferase reporter assay

The transactivation assay was applied according to the manufacturer's protocol (Promega). 10^4 COS-7 cells per well were seeded in 96-well plates in triplicates and incubated for 24 h. Transient transfection was conducted with the reagent TransIT-LT1 (MoBiTec) and the three plasmids pGal5-TK-pGL3 (90 ng), pGal4-hPPARγDEF (9 ng), and pRenilla-CMV (3 ng) in phosphate-buffered saline (PBS). After 7 h of incubation, the cells were treated with the compounds **2a-h**, **3a-h**, or vehicle (DMSO) at selected concentrations and further incubated for 39 h. The medium was removed and it was washed with PBS. Lysis was induced by freezing at −80 °C overnight. To complete lysis a buffer was added and it was shaken for 30 min. Following the protocol, the appropriate reagents were added and luciferase activity was measured with the Multimode Plate Reader EnSpire (PerkinElmer). Renilla luciferase activity served as internal control [26]. The results of the references pioglitazone and telmisartan as well as **2a-h** and **3a-h** are represented by the mean ± SD of ≥3 independent experiments with three replicates each.

Author contributions

The manuscript was written through contributions of all authors. All authors have given approval to the final version of the manuscript.

Declaration of competing interest

The authors declare that they have no known competing financial interests or personal relationships that could have appeared to influence the work reported in this paper.

Acknowledgment

This work was supported by the Austrian Research Promotion Agency FFG [West Austrian BioNMR 858017], the "Tyrolean Cancer Society [Project 17011]", the "Kinderkrebshilfe Südtirol-Regenbogen", and the "Südtiroler Krebshilfe". We thank Christoph Kreutz (Institute of Organic Chemistry, University of Innsbruck) for his assistance in recording ^{13}C NMR spectra and Peter Enoh (Department of Pharmaceutical Chemistry, University of Innsbruck) for technical support.

Appendix A. Supplementary data

Supplementary data to this article can be found online at https://doi.org/10.1016/j.ejmech.2021.113285.

References

[1] D.N. Meenakshi Sundaram, X. Jiang, J.M. Brandwein, J. Valencia-Serna, K.C. Remant, H. Uludağ, Current outlook on drug resistance in chronic myeloid leukemia (CML) and potential therapeutic options, Drug Discov. Today 24 (2019) 1355–1369.
[2] F. Loscocco, G. Visani, S. Galimberti, A. Curti, A. Isidori, BCR-ABL independent mechanisms of resistance in chronic myeloid leukemia, Front. Oncol. 9 (2019) 939.
[3] A. Hoelbl, C. Schuster, B. Kovacic, B. Zhu, M. Wickre, M.A. Hoelzl, S. Fajmann, F. Grebien, W. Warsch, G. Stengl, L. Hennighausen, V. Poli, H. Beug, R. Moriggl, V. Sexl, Stat5 is indispensable for the maintenance of bcr/abl-positive leukaemia, EMBO Mol. Med. 2 (2010) 98–110.
[4] A. Berger, V. Sexl, P. Valent, R. Moriggl, Inhibition of STAT5: a therapeutic option in BCR-ABL1-driven leukemia, Oncotarget 5 (2014) 9564–9576.
[5] J. Wang, L. Lu, C.H. Kok, V.A. Saunders, J.M. Goyne, P. Dang, T.M. Leclercq, T.P. Hughes, D.L. White, Increased peroxisome proliferator-activated receptor γ activity reduces imatinib uptake and efficacy in chronic myeloid leukemia mononuclear cells, Haematologica 102 (2017) 843–853.
[6] B. Yousefi, N. Samadi, B. Baradaran, V. Shafiei-Irannejad, N. Zarghami, Peroxisome proliferator-activated receptor ligands and their role in chronic myeloid leukemia: therapeutic strategies, Chem. Biol. Drug Des. 88 (2016) 17–25.
[7] B. Yousefi, A. Azimi, M. Majidinia, V. Shafiei-Irannejad, R. Badalzadeh, B. Baradaran, N. Zarghami, N. Samadi, Balaglitazone reverses P-glycoprotein-mediated multidrug resistance via upregulation of PTEN in a PPARγ-dependent manner in leukemia cells, Tumor Biol. 39 (2017), 1010428317716501.
[8] S. Prost, F. Relouzat, M. Spentchian, Y. Ouzegdouh, J. Saliba, G. Massonnet, J.-P. Beressi, E. Verhoeyen, V. Raggueneau, B. Maneglier, S. Castaigne, C. Chomienne, S. Chretien, P. Rousselot, P. Leboulch, Erosion of the chronic myeloid leukaemia stem cell pool by PPARγ agonists, Nature 525 (2015) 380–383.
[9] P. Rousselot, S. Prost, J. Guilhot, L. Roy, G. Etienne, L. Legros, A. Charbonnier, V. Coiteux, P. Cony-Makhoul, F. Huguet, E. Cayssials, J.-M. Cayuela, F. Relouzat, M. Delord, H. Bruzzoni-Giovanelli, L. Morisset, F.-X. Mahon, F. Guilhot, P. Leboulch, Pioglitazone together with imatinib in chronic myeloid leukemia: a proof of concept study, Cancer 123 (2017) 1791–1799.
[10] E. Glodkowska-Mrowka, A. Manda-Handzlik, A. Stelmaszczyk-Emmel, I. Seferynska, T. Stoklosa, J. Przybylski, P. Mrowka, PPARγ ligands increase antileukemic activity of second- and third-generation tyrosine kinase inhibitors in chronic myeloid leukemia cells, Blood Cancer J. 6 (2016) e377.
[11] A.M. Schoepf, S. Salcher, P. Obexer, R. Gust, Overcoming imatinib resistance in chronic myelogenous leukemia cells using non-cytotoxic cell death modulators, Eur. J. Med. Chem. 185 (2020) 111748.
[12] A.M. Schoepf, S. Salcher, P. Obexer, R. Gust, Identification and development of non-cytotoxic cell death modulators: impact of sartans and derivatives on PPARγ activation and on growth of imatinib-resistant chronic myelogenous leukemia cells, Eur. J. Med. Chem. 195 (2020) 112258.
[13] A.M. Schoepf, S. Salcher, V. Hohn, F. Veider, P. Obexer, R. Gust, Synthesis and characterization of telmisartan-derived cell death modulators to circumvent imatinib resistance in chronic myeloid leukemia, ChemMedChem 15 (2020) 1067–1077.
[14] M. Goebel, M. Clemenz, B. Staels, T. Unger, U. Kintscher, R. Gust, Characterization of new PPARγ agonists: analysis of telmisartan's structural components, ChemMedChem 4 (2009) 445–456.
[15] V. Obermoser, M.E. Urban, M. Murgueitio, G. Wolber, U. Kintscher, R. Gust, New telmisartan-derived PPARγ agonists: impact of the 3D-binding mode on the pharmacological profile, Eur. J. Med. Chem. 124 (2016) 138–152.
[16] T. Mosmann, Rapid colorimetric assay for cellular growth and survival: application to proliferation and cytotoxicity assays, J. Immunol. Methods 65 (1983) 55–63.
[17] A.B.P. Lopes, E.C. Miranda, V.M.O. Póvoa, B.R. Vergílio, G.C.P. Furlin, M.T. Delamain, G.B. Duarte, C.A. Souza, E.V. De Paula, K.B. Pagnano, Pioglitazone did not affect PPAR-γ, STAT5, HIF2α and CITED2 gene expression in chronic myeloid leukemia patients with deep molecular response, Blood 134 (2019), 1637-1637.
[18] B. Wingelhofer, B. Maurer, E.C. Heyes, A.A. Cumaraswamy, A. Berger-Becvar, E.D. de Araujo, A. Orlova, P. Freund, F. Ruge, J. Park, G. Tin, S. Ahmar, C.-H. Lardeau, I. Sadovnik, D. Bajusz, G.M. Keserű, F. Grebien, S. Kubicek, P. Valent, P.T. Gunning, R. Moriggl, Pharmacologic inhibition of STAT5 in acute myeloid leukemia, Leukemia 32 (2018) 1135–1146.
[19] W. Warsch, K. Kollmann, E. Eckelhart, S. Fajmann, S. Cerny-Reiterer, A. Holbl, K.V. Gleixner, M. Dworzak, M. Mayerhofer, G. Hoermann, H. Herrmann, C. Sillaber, G. Egger, P. Valent, R. Moriggl, V. Sexl, High STAT5 levels mediate imatinib resistance and indicate disease progression in chronic myeloid leukemia, Blood 117 (2011) 3409–3420.
[20] J.W. Jacobberger, R.M. Sramkoski, P.S. Frisa, P.P. Ye, M.A. Gottlieb, D.W. Hedley, T.V. Shankey, B.L. Smith, M. Paniagua, C.L. Goolsby, Immunoreactivity of STAT5 phosphorylated on tyrosine as a cell-based measure of BCR/ABL kinase activity, Cytometry 54 (2003) 75–88.
[21] D.J. Adamson, D. Frew, R. Tatoud, C.R. Wolf, C.N. Palmer, Diclofenac antagonizes peroxisome proliferator-activated receptor-gamma signaling, Mol. Pharmacol. 61 (2002) 7–12.
[22] L.M. Leesnitzer, D.J. Parks, R.K. Bledsoe, J.E. Cobb, J.L. Collins, T.G. Consler, R.G. Davis, E.A. Hull-Ryde, J.M. Lenhard, L. Patel, K.D. Plunket, J.L. Shenk, J.B. Stimmel, C. Therapontos, T.M. Willson, S.G. Blanchard, Functional consequences of cysteine modification in the ligand binding sites of peroxisome proliferator activated receptors by GW9662, Biochemistry 41 (2002) 6640–6650.
[23] R.C. Hui, R.E. Francis, S.K. Guest, J.R. Costa, A.R. Gomes, S.S. Myatt, J.J. Brosens, E.W. Lam, Doxorubicin activates FOXO3a to induce the expression of multidrug resistance gene ABCB1 (MDR1) in K562 leukemic cells, Mol. Cancer Therapeut. 7 (2008) 670–678.
[24] S. Salcher, M. Hermann, U. Kiechl-Kohlendorfer, M.J. Ausserlechner, P. Obexer, C10ORF10/DEPP-mediated ROS accumulation is a critical modulator of FOXO3-induced autophagy, Mol. Cancer 16 (2017) 95.
[25] C. Karnthaler-Benbakka, D. Groza, B. Koblmuller, A. Terenzi, K. Holste, M. Haider, D. Baier, W. Berger, P. Heffeter, C.R. Kowol, B.K. Keppler, Targeting a targeted drug: an approach toward hypoxia-activatable tyrosine kinase inhibitor prodrugs, ChemMedChem 11 (2016) 2410–2421.
[26] E. Raspe, L. Madsen, A.M. Lefebvre, I. Leitersdorf, L. Gelman, J. Peinado-Onsurbe, J. Dallongeville, J.C. Fruchart, R. Berge, B. Staels, Modulation of rat liver apolipoprotein gene expression and serum lipid levels by tetradecylthioacetic acid (TTA) via PPARalpha activation, J. Lipid Res. 40 (1999) 2099–2110.